Chapter 4

Simulation Results

In this chapter, we show the simulation results of the proposed techniques that compare with the conventional spectrum sensing techniques. For easy to understand, we divide our results into four parts following our proposed methods in chapter 3. Four parts of our simulation include the simulation results of DCAED, the simulation results of FSC, the simulation results of two-stage spectrum sensing, and the simulation results of MFSC.

4.1 The simulation results of DCAED

In this section, we firstly give the performance evaluation of two types of conventional energy detection techniques (CDR and CFAR) and ATED. Then, we compare the performance of these techniques to DCAED. Additive white Gaussian noise (AWGN) channel with SNR between -25 to 0 dB is considered as the communication channel of our simulation. The primary user signal is considered as i.i.d. process. The performance of spectrum sensing techniques are evaluated through 100,000 Monte Carlo simulation. The parameters in the simulation are as follows: $\mathbf{N}$= 1000, $\mathbf{P_d}$=0.9 and $\mathbf{P_{fa}}$=0.01. In addition, noise variance is assumed to be estimated by the secondary user. All the experiments are performed under Windows 8.1 and MATLAB running on a PC equipped with an Intel Core i7 CPU at 3.40 GHz and 32 GB RAM memory.

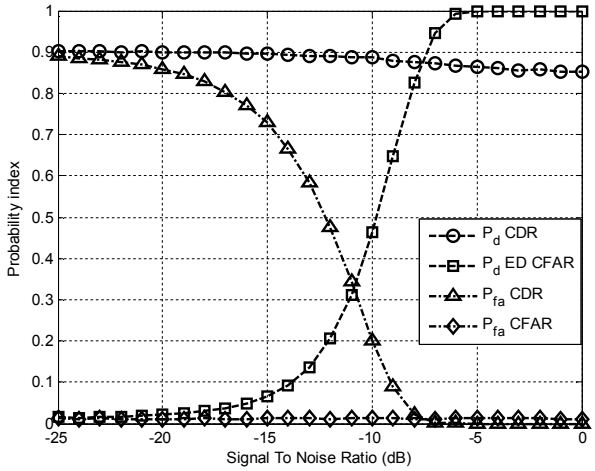

Figure 4-1 Probability of detection and probability of false alarm versus SNR of CDR and CFAR.

Figure 4-1 shows the performance of both P_{fa} and P_d versus SNR of communication channel. The simulation results prove that CDR technique gives high detection performance for all range of SNR. As mentioned in section I, there is always be tradeoff on detection performance (high P_d) by fixing only a single target performance metric. The threshold based on CDR gives high P_{fa} at low SNR. Although the CFAR technique gives low P_{fa} for all range of SNR, it also gives poor detection performance at low SNR levels.

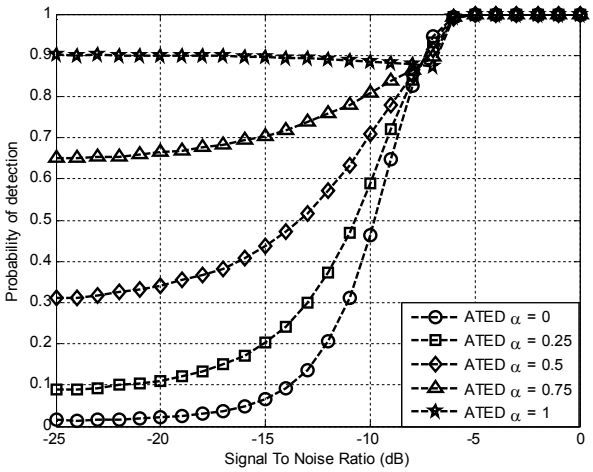

Figure 4-2 Probability of detection versus SNR of ATED.

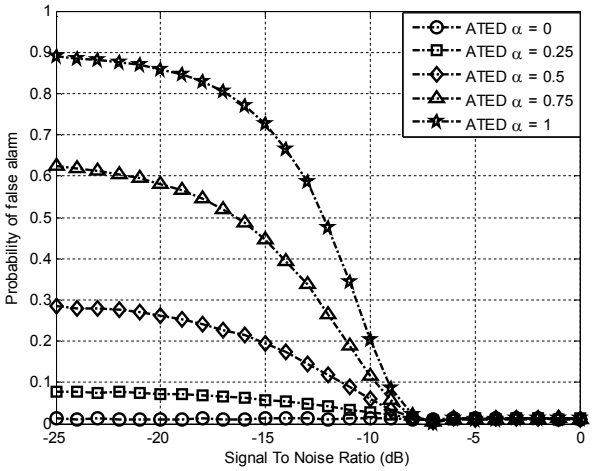

Figure 4-3 Probability of false versus SNR of ATED technique.

Figure 4-2 and Figure 4-3 show the performance of ATED with different in adaptive parameter value in terms of P_d and P_{fa}, respectively. The simulation results show that ATED$_{\alpha=1}$ gives high probability of detection for all range of SNR as the same as CDR technique. In perspective of probability of false alarm, ATED$_{\alpha=1}$ gives high P_{fa} at low SNR. On the contrary, ATED$_{\alpha=0}$ gives low probability of false alarm for all range of SNR as the same as CFAR

technique. However, ATED$_{\alpha=0}$ gives low probability of detection at low SNRs. In addition, if we set the value of adaptive parameter between 0 to 1, the performance of ATED is between CFAR and CDR.

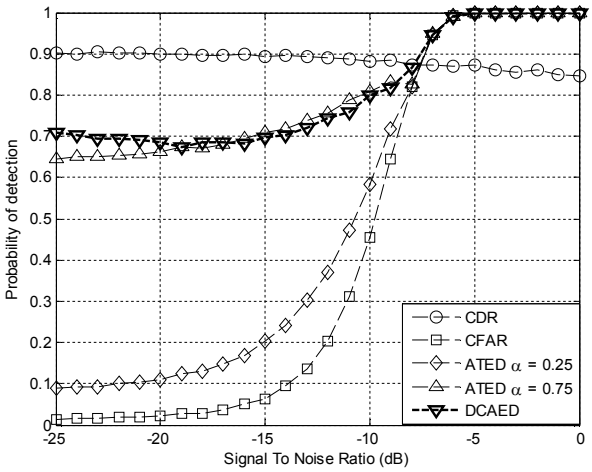

Figure 4-4 Probability of detection of the DCAED as compared to ATED, CDR and CFAR.

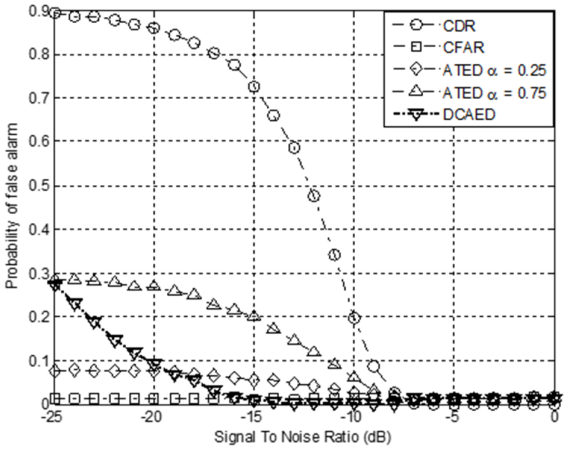

Figure 4-5 Probability of false alarm of the DCAED as compared to ATED, CDR and CFAR

DCAED changes the threshold under different condition of communication channel controlled by the adaptive factor. The adaptive factor is derived from the critical sample of the system which retains the interdepedent between P_{fa} and P_d. Thus, we can conclude that the threshold of DCAED is adapted controlled by P_{fa} and P_d. depending on the condition of icommunication channel. Figure 4-4 compares the probability of detection of the DCAED to ATED$_{\alpha=0.75,}$ ATED$_{\alpha=0.25}$, CDR and CFAR. The simulation results show that DCAED gives higher P_d than ATED$_{\alpha=0.75,}$ ATED$_{\alpha=0.25}$ and CFAR. On the other hand, the DCAED technique gives higher P_d than CDR techniqe when SNR is higher than-8 dB. As show in Figure 4-5, DCAED gives lower

P_{fa} than ATED$_{\alpha=0.75}$ and CDR. DCAED technique meets the spectrum sensing requirement of IEEE 802.22 when SNR is higer than -20 dB which the spectrum sensing technique has to perform spectrum sensing with probability of false detection less than 0.1.

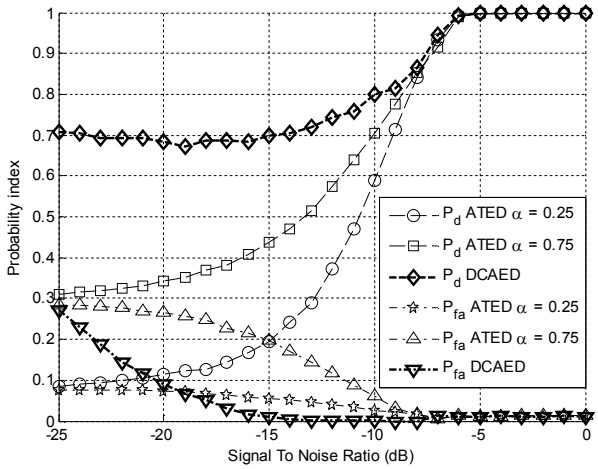

Figure 4-6 Tradeoff in an accuracy of detection of the DCAED as compared to ATED.

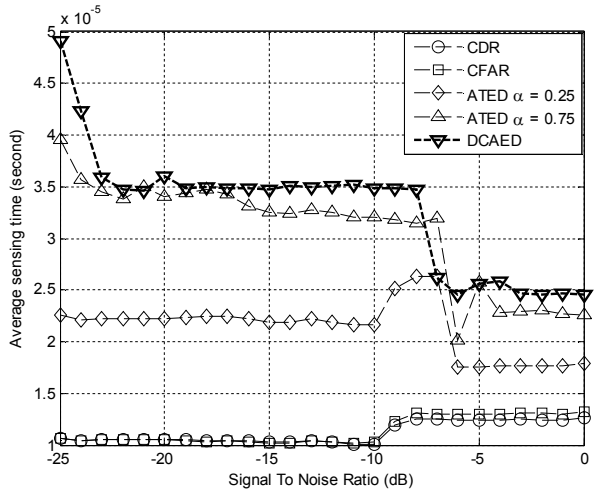

Figure 4-7 Average sensing time of the DCAED as compared to ATED, CDR and CFAR.

Figure 4-6, shows the tradeoff in an accuracy of detection of the DCAED as compared to ATED. The simulation results prove that DCAED overcomes demerits of the tradeoff in the accuracy of detection of ATED. Although DCAED gives higher P_{fa} than ATED$_{\alpha=0.25}$, DCAED gives much higher P_d than ATED$_{\alpha=0.25}$ and ATED$_{\alpha=0.75}$. In addition, the estimated noise variance is used to select the adaptive factor. The adaptive factor under high SNR condition can be computed with less complexity than adaptive factor under low SNR condition. Thus, the DCAED consumes less time in performing spectrum sensing under high SNR condition (as shown in Figure 4-7). The sensing time of DCAED highly achieves the requirement of the IEEE 802.22 standard which is less than 2 seconds. Although the DCAED spends more sensing time

than the other technique, the DCAED outperform the tradeoff in an accuracy of detection which is the main disadvantage of the other techniques.

4.2 The simulation results of FSC

4.2.1 Preliminary

In this section, we evaluate the performance of six conventional spectrum sensing techniques — ED, MED, CAV, MME, MFD, and LED — under the assumption that a received WM signal has a randomly occurring pattern. Two important factors — P_{d} and sensing time of each technique — are considered in our performance evaluation.

With an aim to study spectrum sensing performance under different levels of knowledge, the SU is equipped with four different knowledge bases of wireless microphone (WM) signal as described in Table 4-1.

The simulation results of six conventional spectrum sensing techniques — ED, MED, CAV, MME, MFD, and LED — are shown in Table 4-2. As four of the six techniques — ED, MED, CAV, and MME — are blind techniques, their detection performances will not be affected by different knowledge bases. Hence, the individual results of these blind techniques are not shown; rather, they are shown collectively due to the fact that they have similar detection performances. On the other hand, different knowledge bases greatly affect the detection performances of the knowledge-based techniques — MFD and LED. Results on four cases are shown in details.

Table 4-1 Different knowledge bases of PU signal known to an SU.

Case	Description
1	Silent of WM signal is known by SU
2	Soft speaker of WM signal is known by SU
3	Loud speaker of WM signal is known by SU
4	All three patterns of WM signals are known by SU

Figure 4-8 shows the simulation results of MFD and LED for the four cases outlined in Table 4-1. The graph plots P_{d} as a function of SNR. It is clear that the detection performance of MFD is greatly affected by the knowledge base of PU's signal. When SU observes a pattern of WM signal that is not in the knowledge base, the detection performance of MFD greatly degrades.

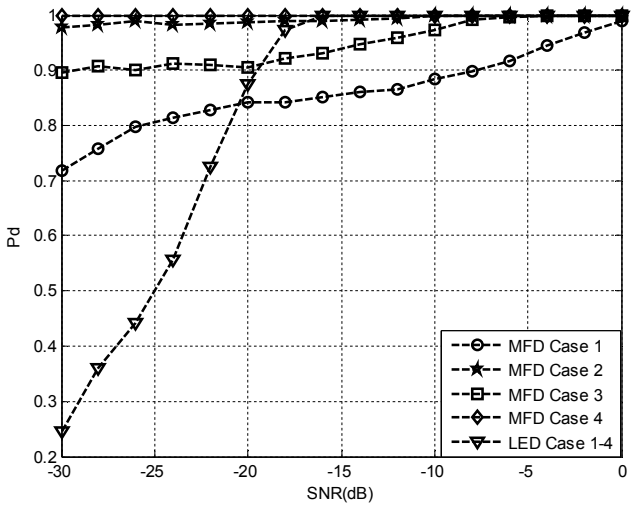

Figure 4-8 Detection performance of MFD and LED under different received wireless microphone signal cases.

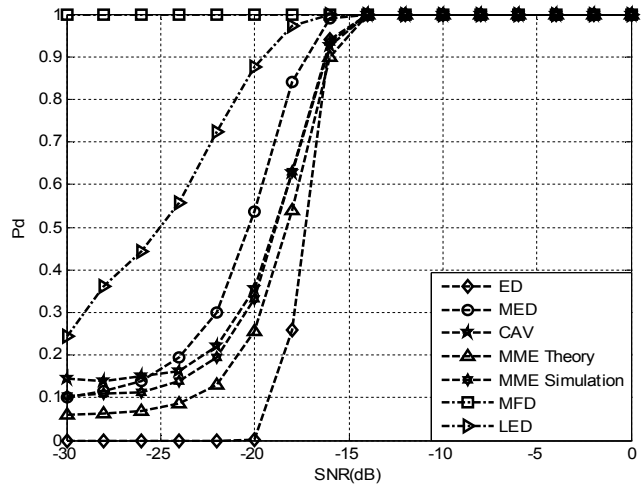

Figure 4-9 Performance comparison of conventional spectrum sensing techniques when the patterns of the PU signal are known.

As depicted in the figure, the detection performance of LED in cases 1–4 is shown using only a single line. This is because the detection performances were practically identical to each other, due to the fact that the leading eigenvectors of the WM signal patterns were similar to each other. Thus, the detection performance of LED was not affected by a difference in WM signal pattern. However, LED inflicts a high computational burden upon the SU when performing spectrum sensing; thus, the associated sensing time is often substantial.

Figure 4-9 shows the performance comparison of conventional spectrum sensing techniques when the patterns of WM signals are known. MFD offers the best detection

performance among the spectrum sensing techniques. When evaluating the performance of MME, the calculated MME threshold (theoretical), γ_{MME}, offer an implausible performance at low SNRs.

In [54], the authors improve the detection performance of MME by finding new thresholds through Monte Carlo simulations. To compare the performance of MME under the different types of thresholds (theoretical and Monte Carlo simulations), we present the performance of "MME Theory" and "MME Simulation" in Figure 4-9. Note that "MME Theory" denotes experimental results where the threshold is calculated from a theoretical formula. "MME Simulation" denotes experimental results where the threshold is estimated through Monte Carlo simulations.

Table 4-2 gives a performance comparison of conventional spectrum sensing techniques for various cases of prior knowledge. The SNR required of a spectrum sensing technique to meet the required accuracy of detection (that is, $P_{\mathrm{d}} \geq 0.9$) [43], is given in the "Critical SNR" column of Table 4-2. The lower the "Critical SNR" value, the more tolerant to noise the technique is. From Table 4-2, the knowledge-based spectrum sensing techniques — MFD and LED— are confirmed to be more tolerant to noise than the blind techniques.

On the other hand, the average sensing time shown for each technique is based on the average from the Monte Carlo simulations. As shown in Table 4-2, ED consumes the least average sensing time, whereas LED consumes the longest average sensing time. These average sensing time values are used as a benchmark when evaluating the average sensing time of the FSC algorithm.

Moreover, the results in Table 4-2 show that ED offers the maximum number of channels per sensing period. However, there is no standard or requirement that defines the minimum number of channels that should be monitored in a given sensing period. If the number of channels per sensing period increases, then the SU will have more opportunities to utilize the unused licensed band.

Table 4-2 Performance comparison of conventional spectrum sensing techniques.

Sensing technique			Prior knowledge			Ability to detect wireless microphone signal		
			Waveform pattern	Noise power	Memory (Kbytes)	Critical SNR ($P_d \geq 0.9$)	Average sensing time (ms)	Channels/Sensing period of 2 seconds
Blind spectrum sensing	ED		✗	✓	0	-16 dB	0.04997	3,602
	MED		✗	✓	0	-16 dB	2.6	69
	CAV		✗	✗	0	-16 dB	2.5	72
	MME		✗	✗	0	-16 dB	2.9	62
Spectrum sensing based on prior knowledge	MFD	Case 1	✓	✓	40	-8 dB	2.5	72
		Case 2	✓	✓	40	-30 dB	2.5	72
		Case 3	✓	✓	40	-30 dB	2.5	72
		Case 4	✓	✓	120	-30 dB	5.4	33
	LED	Case 1	✓	✓	0.192	-18 dB	78.09	2
		Case 2	✓	✓	0.064	-18 dB	78.09	2
		Case 3	✓	✓	0.064	-18 dB	78.09	2
		Case 4	✓	✓	0.192	-18 dB	80.7	2

4.1.2 Simulation Results

In this section, we give the simulation results of eight spectrum sensing techniques. The transmitted PU signals are assumed to be WM signals, based on IEEE 802.22, whereby the patterns of the WM signals are assumed to be in the knowledge base of the SU. The parameters of the WM signals are shown in Table 4-1. A single received WM signal is assumed to contain one of three randomly occurring patterns. The communication channel between the transmitter and the receiver is assumed to be an AWGN channel, and the SNR at the receiver is assumed to be between -30 dB and 0 dB. The other parameters that were used in the simulations took the following values: n= 5,000; L= 10; and P_{fa} = 0.1. All the experiments are performed under Windows 7 and MATLAB running on a PC equipped with an Intel Dual-Core CPU at 2.93 GHz and 4 GB RAM memory.

As depicted in Figure 4-10, the FSC algorithm gives a better detection performance than other conventional spectrum sensing techniques, except MFD, which is known as the optimum spectrum sensing technique. The critical SNR of the FSC algorithm is -24 dB (see Table 4-3). From the perspective of sensing time, the FSC algorithm consumes less sensing time than the other conventional techniques, except ED (see Table 4-3). The reason for this is that the FSC algorithm performs spectrum sensing with little computational burden due to the small size of the weight vector ($\hat{\mathbf{x}}$). Calculated from the averaged sensing time of FSC, the FSC algorithm can sense 3,370 channels per sensing period. When compared

with the results in Table 4-2, we can see that the FSC algorithm can perform spectrum sensing with a number of communication channels that rivals that of ED.

To validate the performance of the FSC algorithm, graphs of $P_{\mathrm{d(FSC)}}$, $P_{\mathrm{m(FSC)}}$, and $P_{\mathrm{fa(FSC)}}$ are shown in Figure 4-11(a). In this figure, as SNR increases, $P_{\mathrm{d(FSC)}}$ increases while $P_{\mathrm{m(FSC)}}$ and $P_{\mathrm{fa(FSC)}}$ decrease. The simulation results are as we expected, and this is explained as follows. By projecting the received signal to the proposed coordinate system, we obtained the weight vector and weight of correspondence between the received signal and the coordinate system. We found that the weight vector effectively represents the WM signal especially when SNR is higher than -18 dB. When SNR is lower than -18 dB, where noise power is much greater than the WM signal power, the weight vector is contaminated with noise. Hence, the magnitude of the weight of correspondence between the received signal and the coordinate system is lower than the predetermined FSC threshold, which causes misdetection.

However, $P_{\mathrm{d(FSC)}}$ is still higher than the P_{d}s of other conventional techniques, including ED, MED, CAV, MME, and LED. This is because the effect of the noise on the weight vector is less than that on the WM signal.

To evaluate the tradeoff between $P_{\mathrm{m(FSC)}}$ and $P_{\mathrm{fa(FSC)}}$, $P_{\mathrm{m(FSC)}}$ is plotted as a function of $P_{\mathrm{fa(FSC)}}$, as shown in Figure 4-11(b). It should be noted that $P_{\mathrm{m(FSC)}}$ is greater than 0 when the SNR is lower than -18 dB; hence, $P_{\mathrm{m(FSC)}}$ at three different SNRs — -20 dB, -26 dB, and -30 dB — is shown. From Figure 4-11(b), it can be seen that $P_{\mathrm{m(FSC)}}$ slightly decreases when $P_{\mathrm{fa(FSC)}}$ increases, which is similar to what happens in the cases of the other conventional techniques.

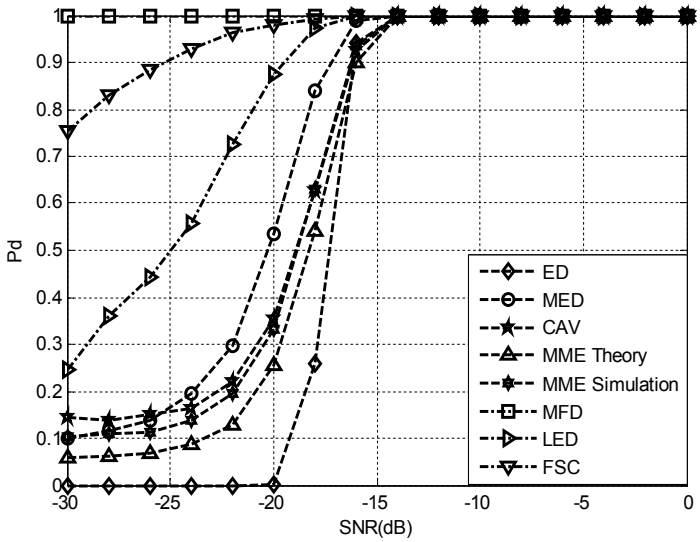

Figure 4-10 Probability of detection vs. SNRs of ED, MED, CAV, MME, MFD, LED, and FSC.

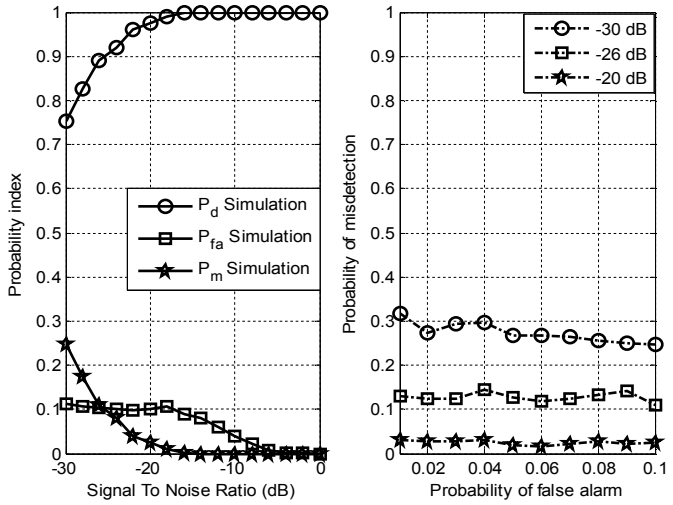

(a) (b)

Figure 4-11 Performance of FSC algorithm.

Table 4-3 Comparison of critical SNR and average sensing time (case 4).

Sensing technique		Critical SNR ($P_{\mathrm{d}} \geq 0.9$)	Average sensing time (ms)
Blind spectrum sensing	ED	-16 dB	0.0499
	MED	-16 dB	2.6
	CAV	-16 dB	2.5
	MME	-16 dB	2.9
Spectrum sensing based on prior knowledge	MFD	-30 dB	5.4
	LED	-18 dB	30.7
	FSC	-24 dB	0.0534

To evaluate the overall performances of the spectrum sensing techniques, we combine two performance metrics, P_{d} and average sensing time of each technique, using a standard multi-criteria ranking technique — analytic hierarchy process (AHP) [30]. In the first step, we have to determine the importance ratio between P_{d} and average sensing time, which has never been standardized. Herein, the importance ratios are set as follows: 1:7, 1:5, 1:3, 1:2, 1:1, 2:1, 3:1, 5:1, and 7:1. It should be noted that the importance ratio of 1:7 means that the P_{d} is 7 times more important than the average sensing time, while 7:1 means the P_{d} is 7 times less important than the average sensing time. As shown in Figure 4-12, the FSC algorithm gives the highest overall performance at any weight of importance. The reason is that the FSC algorithm gives a high rate of detection while utilizing a short sensing time.

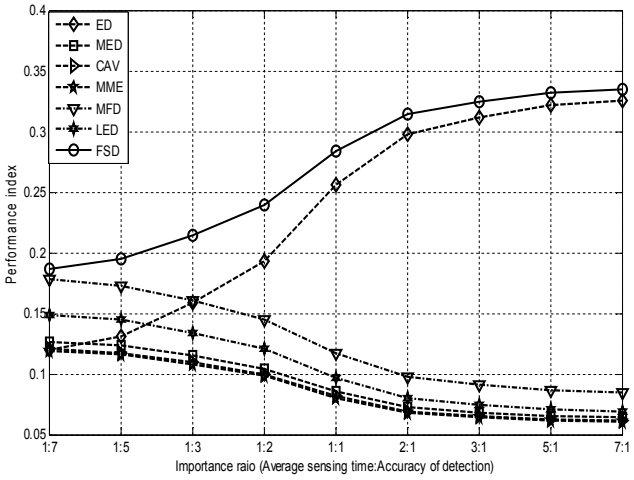

Figure 4-12 Performance comparison using AHP algorithm.

4.3 The simulation of two-stage spectrum sensing

In our proposed schemes, there are 2 main parameters that have to be considered, including $\mathrm{P_{fa}}$ and L. Threshold of the proposed techniques can be found by using (2-21), (2-28) and (3-45). Since these parameters relate to each other and also affect to the performace of the proposed techniques, these parameters need to change simultaneously. Figure 4-13 and Figure 4-14 show the probability of detection and the average sensing time as a function of SNR with difference in smoothing factors when noise power uncertainty occurs (β = 2 dB) and $\mathrm{P_{fa}}$=0.1, respectively. As shown in the figures, two-stage spectrum sensing techniques offer more reliable detection under noise power uncertainty factor equal to 1 when the smoothing factor increaes. However, an increase in the smoothing factor causes these techniques consume more time in performing spectrum sensing.

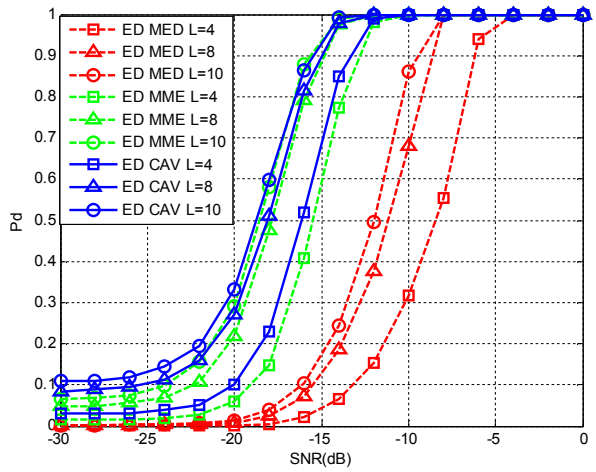

Figure 4-13 Probability of detection versus SNR of two-stage spectrum sensing techniques with difference in smooting factors (L) when the uncertainty of noise power occur (β =2 dB) and P_{fa}=0.1.

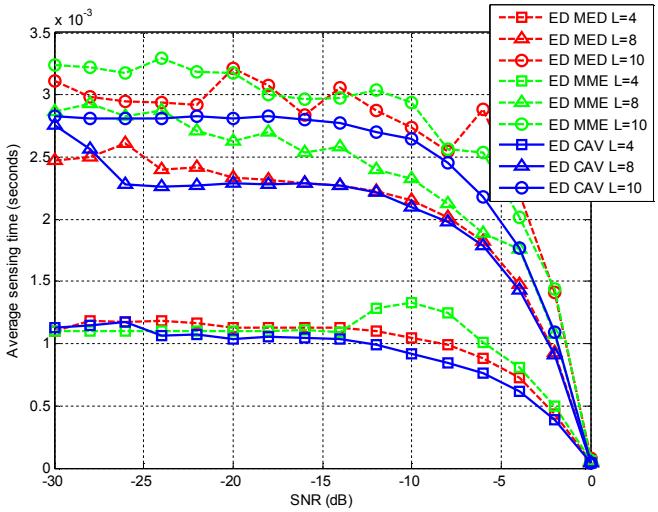

Figure 4-14 Average sensing time versus SNR of two-stage spectrum sensing techniques with difference in smooting factors (L) when the uncertainty of noise power occur (β =2 dB) and P_{fa}=0.1.

Figure 4-15 and Figure 4-16 show the probability of detection and the average sensing time as a function of SNR with difference in smoothing factors when noise power uncertainty occurs (β = 2 dB) and P_{fa}=0.2, respectively. As mentioned earlier, an increase in smoothing factor makes these techniques more time consuming in performing spectrum sensing. By comparing Figure 4-13 and Figure 4-15, two-stage spectrum sensing techniques offer more reliable detection when the smoothing factor is eqaul to 10 and P_{fa}=0.2. Although the smoothing factor equal to 10 makes two-stage spectrum sensing techniques more time consuming in performing spectrum sensing, the primary user can ensure that it is protected from harmful interference caused by the secondary user.

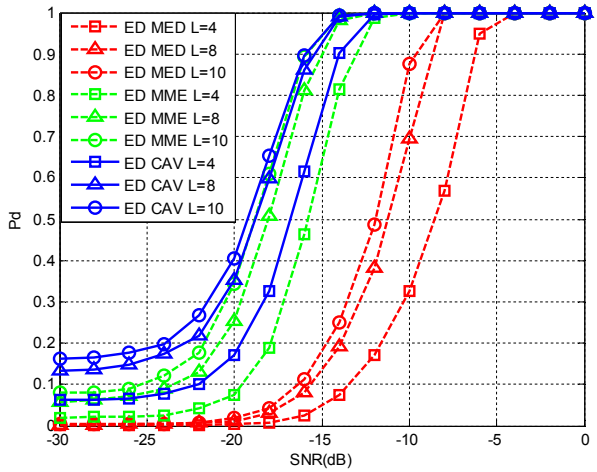

Figure 4-15 Probability of detection versus SNR of two-stage spectrum sensing techniques with difference in smooting factors (L)
when the uncertainty of noise power occur (β =2 dB) and P_{fa}=0.2.

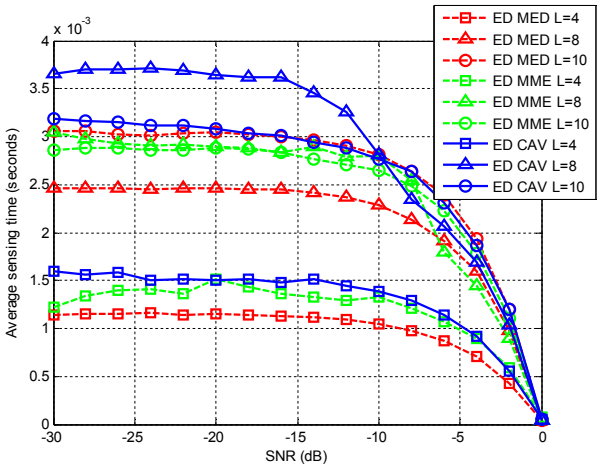

Figure 4-16 Average sensing time versus SNR of two-stage spectrum sensing techniques with difference in smooting factors (L)
when the uncertainty of noise power occur (β =2 dB) and P_{fa}=0.2.

Figure 4-17 and Figure 4-18 show the probability as a function of SNR when noise power uncertainty factor (β) equal to 1 and 2 dB, respectively. Figure 4-19 and Figure 4-20 show the average sensing time as a function of SNR when noise power uncertainty factor (β) equal to 1 and 2 dB, respectively. Simulation results proved that the proposed of ED to CAV two-stage spectrum sensing technique offers detection performance nearly to CAV technique. However, at high SNRs environment, the proposed of ED to CAV two-stage spectrum sensing technique uses less sensing time than CAV. From the simulation results, the proposed of ED

to CAV two-stage spectrum sensing technique offers an accurate performance when smoothing factor L=10 and P_{fa}=0.2. Even though the proposed technique takes the longest time in the sensing period, it offers much more reliable detection than the others. It is worth using this period of time to protect the primary user from harmful interference caused by the secondary user.

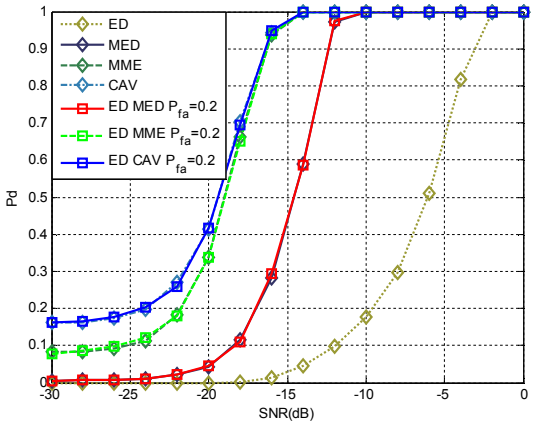

Figure 4-17 Probability of detection versus SNR when the uncertainty of noise power occur (β =1 dB).

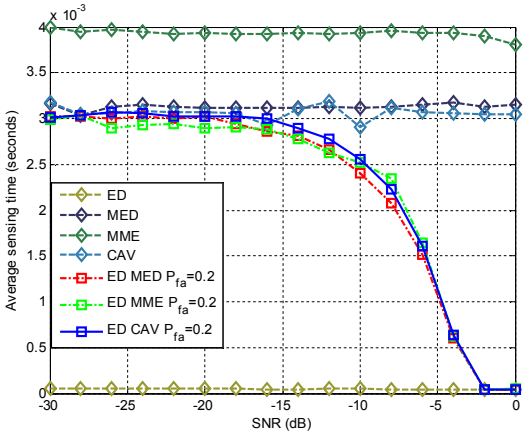

Figure 4-18 Average sensing time versus SNR when the uncertainty of noise power occur (β =1 dB).

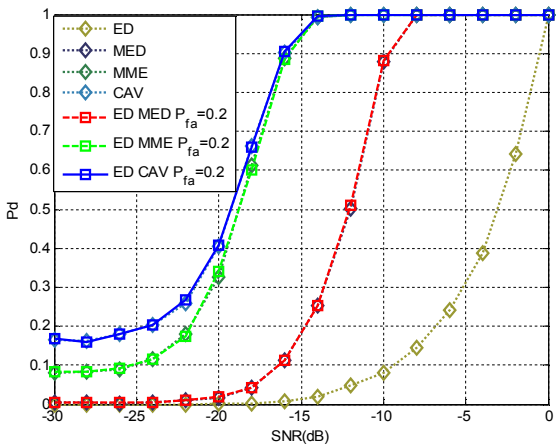

Figure 4-19 Probability of detection versus SNR
when the uncertainty of noise power occur (β =2 dB).

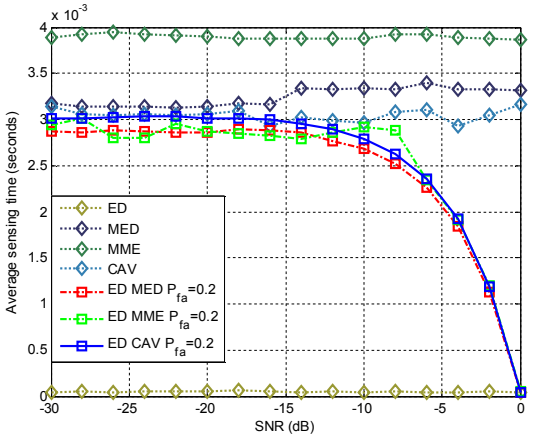

Figure 4-20 Average sensing time versus SNR
when the uncertainty of noise power occur (β =2 dB).

4.4 The simulation results of MFSC

In this section, we give the performance comparison of MFD, LED, MFSC algorithm for additive white Gaussian noise (AWGN) channel under noise uncertainty and path loss effect when a random occurring pattern of WM signal is considered as the PU signal. The distance (d) between WM device and the SU is set within the range of 10 to 1000 meters. The loss constant (C) is set be 0.00031623, then the received signal power is -95 dBm at 100 m [43]. The noise uncertainty factor (B) is between 0 to 2 dB [75]. It should be noticed that when B is 0 means that the noise uncertainty does not occur. Other parameters are setting as follows: $N = 5000$, $\aleph = 2$, $P_{\mathrm{d}} = 0.9$ and $P_{\mathrm{fa}} = 0.01$. All the experiments are done by using MATLAB and averaged on 10,000 Monte-Carlo realizations.

As shown in Figure 4-21, MFD gives the highest P_{d} among these techniques. In perspective of P_{d}, MFD meets the spectrum sensing requirement, which P_{d} should greater than or equal to 0.9, when *d* is less than 650 m. However, P_{fa} of MFD does not meet the requirement, which P_{fa} should less than 0.1, at any distance. This means that the PU is greatly protected from interference caused by SU. However, the SU has a high probability to lose the opportunities to utilize the available spectrum band. On the other hand, MFSC algorithm meets the requirement in perspective of P_{d} with shorter distance. Nevertheless, MFSC meets the requirement in perspective of P_{fa} for all distances. For LED, it gives the worst detection performance when compared to the others. As shown in Figure. 4-22, MFSC algorithm consumes much less sensing time than the others. During the evaluation, we also correct the space of database requirement of these techniques. We found that LED requires much less space of database when it consumes only 0.197 Kbytes while MFD and MFSC require 120 and 80 Kbytes, respectively.

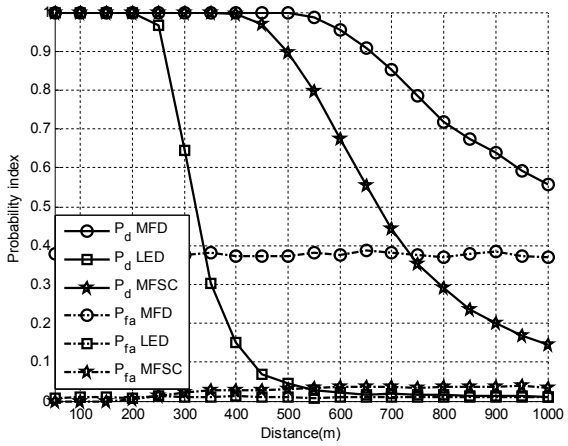

Figure 4-21. Performance comparison of MFD, LED and MFSC when B is 0.

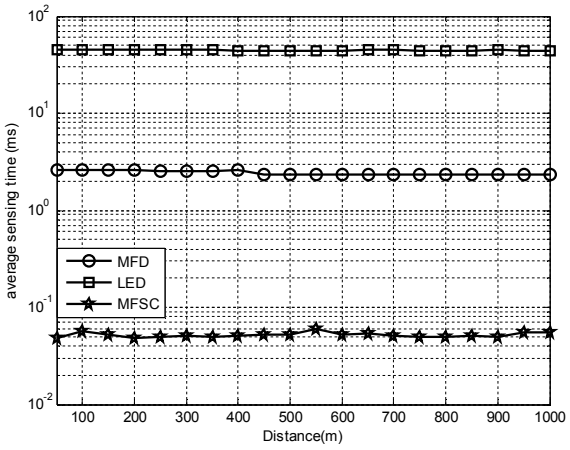

Figure 4-22 Average sensing time of MFD, LED and MFSC when B is 0.

Figure 4-23 compares the detection performance when *B* is 1. As a results, MFD

still gives the highest P_{d}. However, P_{fa} is now less than 0.1. This is because there is an uncertain in noise power which the power may less than the estimated noise power. It means that the effect of noise is lower and then it is easy to distinguish between PU signal and noise. On the other hand, the performance LED and MFSC algorithm, which perform spectrum sensing under framework of PCA algorithm, are nearly the same as when noise uncertainty does not occur. In perspective of average sensing time (as shown in Figure. 4-24), MFSC algorithm still consumes the least average sensing time.

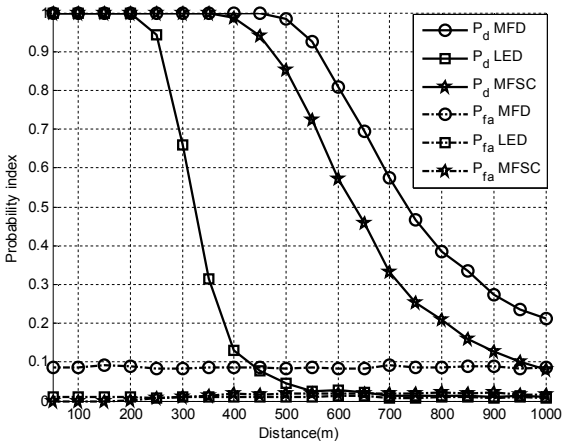

Figure 4-23 Performance comparison of MFD, LED and MFSC when B is 1.

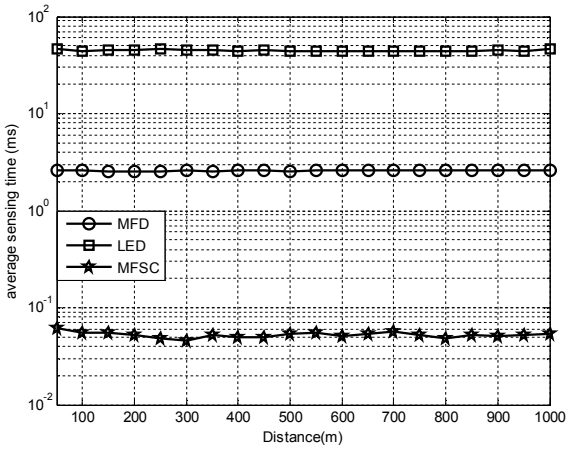

Figure 4-24 Average sensing time of MFD, LED and MFSC when B is 1.

As shown in Figure 4-25, the detection performance of MFSC algorithm is now nearly to MFD because the occurrence of noise uncertainty greatly degrades the detection performance of MFD but does not degrade the detection performance of MFSC algorithm. MFSC algorithm gives higher P_{d} than MFD when the distance is greater than 600 m. This means that when the strength of PU signal is attenuated by path loss together with the increasing in an effect of noise uncertainty, matched filter lose its ability to measure the similarity between received signal and a known PU signal, which is kept in the database,

and cannot distinguish them. For LED, it gives the worst detection performance among these techniques. However, we can noticed that LED is the most robustness techniques to the occurrence of noise uncertainty because it gives the same P_{d} even the strength of noise uncertainty increases. As shown in Figure 4-26, the average sensing time of these techniques are the same as when B is 0 or 1.

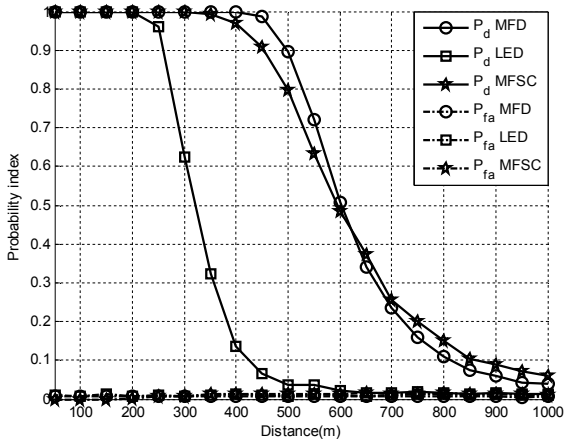

Figure 4-25 Performance comparison of MFD, LED and MFSC when B is 2.

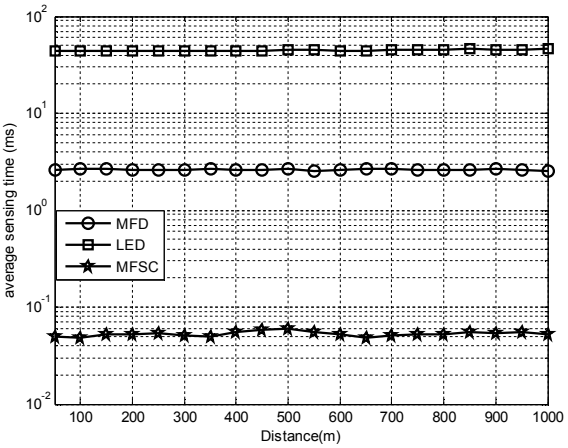

Figure 4-26 Average sensing time of MFD, LED and MFSC when B is 2

From the simulation results, MFD offers the best detection performance in perspective of P_{d}. However, MFD does not meet the spectrum sensing requirement in perspective of P_{fa} at any distance when noise uncertainty does not occur. Moreover, the occurrence of noise uncertainty greatly degrades the detection performance of MFD. On the other hand, MFSC algorithm gives better detection performance than LED but worse than MFD. MFSC algorithm is more robust to the occurrence of noise uncertainty than MFD. In addition, MFSC algorithm gives higher P_{d} than MFD when the distance is greater than 600 m together with 2 dB of noise uncertainty factor (B). In perspective of average sensing time, MFSC algorithm consumes the least average sensing time for all noise

uncertainty factors (B) and distances. For LED, it is the most robustness techniques to the occurrence of noise uncertainty and requires much less space database than the others.